united nations educational, scientific and cultural organization

international atomic energy agency

the
abdus salam
international centre for theoretical physics

SMR.1313 - 8

Summer Colloquium on the Physics of Weather and Climate

Workshop on
Land-Atmosphere Interactions in Climate Models
(28 May - 8 June 2001)

The Surface Energy and Water Balances in a Semi-Arid Climate

Christopher M. Taylor
Centre for Ecology and Hydrology Wallingford
Crowmarsh Gifford, Oxfordshire
OX10 8BB Wallingford
U.K.

The Surface Energy and Water Balances in a Semi-Arid Climate

(i) Semi-Arid Climates

(ii) HAPEX-Sahel

(iii) Diurnal Variability

(iv) Daily Variability

(v) Seasonal Variability

(vi) Interannual Varibility

Reference List

1. Allen SJ, Wallace JS, Gash JHC, et al: Measurements of albedo variation over natural vegetation in the Sahel. Int.J.Climatol. 1994;14:625-636.

2. Allen SJ, Grime VL: Measurements of transpiration from savanna shrubs using sap flow gauges. Agric.For.Met. 1995;75:23-41.

3. Cox PM, Huntingford C, Harding RJ: A canopy conductance and photosynthesis model for use in a GCM land surface scheme. J.Hydrol. 1998;212-213:79-94.

4. Cox PM, Betts RA, Bunton CB, et al: The impact of new land surface physics on the GCM simulation of climate and climate sensitivity. Clim.Dyn. 1999;15:183-203.

5. Gaze SR, Brouwer J, Simmonds LP, et al: Dry season water use patterns under Guiera senegalensis L. shrubs in a tropical savanna. Journal Of Arid Environments 1998;40:53-67.

6. Goutorbe JP, Lebel T, Tinga A, et al: HAPEX-Sahel - a large-scale study of land-atmosphere interactions in the semi-arid tropics. Ann.Geophys. 1994;12:53-64.

7. Hanan NP, Prince SD: Stomatal conductance of West-Central Supersite vegetation in HAPEX-Sahel: Measurements and empirical models. J.Hydrol. 1997;189:536-562.

8. Huntingford C, Allen SJ, Harding RJ: An intercomparison of single and dual-source vegetation-atmosphere transfer models applied to transpiration from Sahelian savannah. Boundary-Layer Meteorol. 1995;74:397-418.

9. Mahfouf JF, Noilhan J: Comparative-study of various formulations of evaporation from bare soil using insitu data. J.Appl.Meteorol. 1991;30:1354-1365.

10. Taylor CM, Saïd F, Lebel T: Interactions between the land surface and mesoscale rainfall variability during HAPEX-Sahel. Mon.Weath.Rev. 1997;125:2211-2227.

11. Taylor CM: The influence of antecedent rainfall on Sahelian surface evaporation. Hydrol.Processes 2000;14:1245-1259.

12. Taylor CM, Blyth EM: Rainfall controls on evaporation at the regional scale: An example from the Sahel. J.Geophys.Res.Atmos. 2000;105:15469-15479.

13. Zeng N, Neelin JD, Lau KM, et al: Enhancement of interdecadal climate variability in the Sahel by vegetation interaction. Science 1999;286:1537-1540.

A Useful Web Site is the HAPEX-Sahel database – it contains much of the data shown in this lecture and much more besides: http://www.ird.fr/hapex

Map 6 Aridity Zones

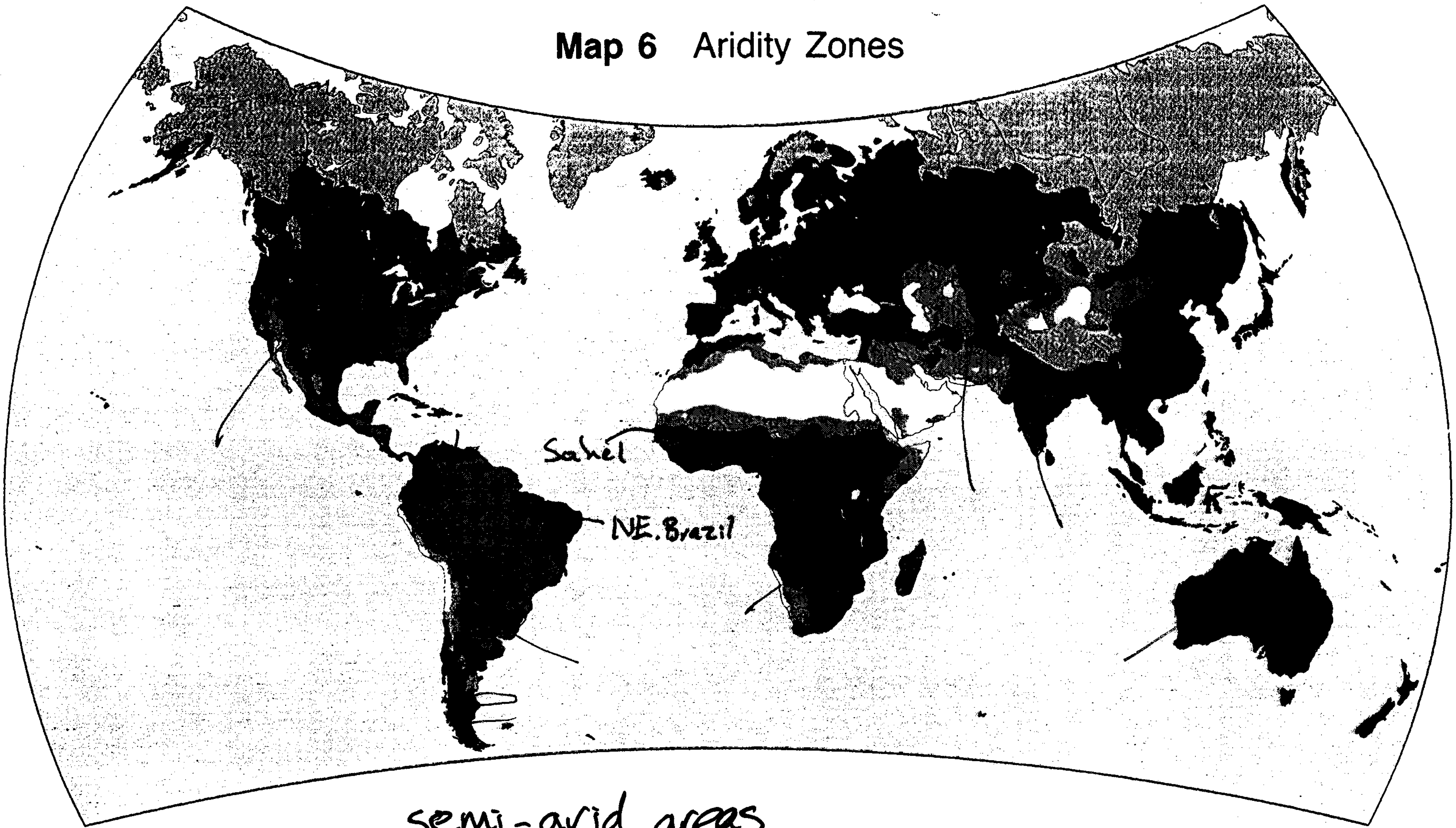

semi-arid areas

$20\% \leq P/PET \leq 50\%$

P = Annual Precipitation

PET = Annual Potential Evapotranspiration

semi-arid areas cover 17.7% of land globally

- Hyperarid
- Arid
- Semiarid
- Dry subhumid
- Humid
- Cold climates

UNEP World Atlas of Desertification

Source: CRU/UEA, UNEP/GRID

CLIMATIC VARIABILITY IN DRYLANDS

Introduction

The study of desertification is hampered by the normal variability of dryland areas, as outlined briefly in the Introduction. Accurate indentification of the causes of desertification, and thus suitable strategies for its treatment, can only be made by paying close attention both to the human use and possible mismanagement of resources and also to the way in which dryland ecosystems and their resources respond to climatic variations. While this atlas concentrates on human-induced soil degradation, it is important to note the dynamic nature of some of the natural environmental elements in the dryland equation.

The inherent variability of dryland environments is very largely governed by the variations in climatic parameters that characterize such regions. Chief among these climatic parameters is precipitation, the input of moisture into the desert ecosytem. While many dryland areas receive important inputs of moisture from dew, and some others from fog, rainfall is the key source of moisture in most of the world's dryland regions. However, the "effectiveness" of rainfall, that is the amount available for plant growth or other uses, is also dependent upon the main output from the ecosystem, evapotranspiration, which is governed by parameters such as vegetation cover and type, wind speeds, and perhaps most importantly temperature. Hence in this section a closer look will be made at the variability of rainfall and temperature in the world's drylands as a contextual background to the preceding pages on dryland degradation. The graphs and maps shown on these pages are supplied by the CRU.

Rainfall

Figures 1 to 3 show time series graphs of annual rainfall for three dryland regions: the Sahel from the Atlantic coast to 35°E; the northeastern region of Brazil from 44°W to the Atlantic coast and from the Equator to 10°S, and North China from 100°E to the China Sea coast and from the borders with Mongolia and Russia to 35°N.

The graphs for each area have been derived as follows: the annual rainfall series for each station in the area is normalized by taking away the long-term mean from each value and the difference is then divided by the long-term standard deviation. The long-term period on which the mean and standard deviation are based in each area is 1951–1980, the period of the climate surfaces used for the annual Aridity index which has given the dryland area boundaries throughout the global and continental Africa sections of this atlas.

Normalizing gives a set of data series that are more readily comparable as each series will then have a mean close to zero and a standard deviation close to one. The spatial mean rainfall anomalies are then found by averaging the values for all stations in the area with data. Although the number of stations with

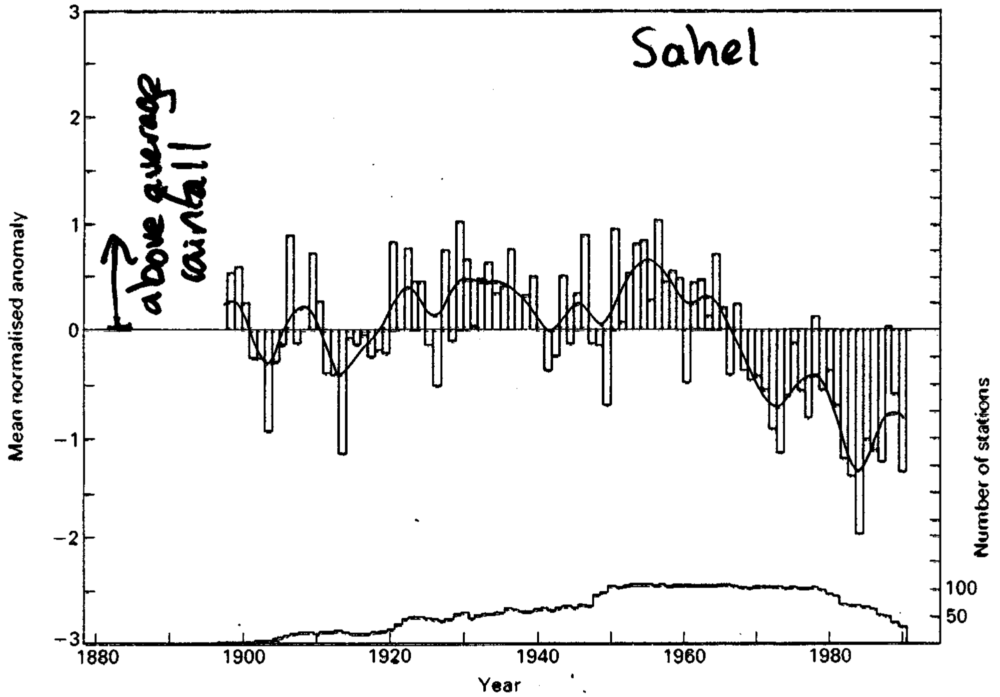

Figure 1 Time series of annual rainfall – The Sahel (1897–1990)

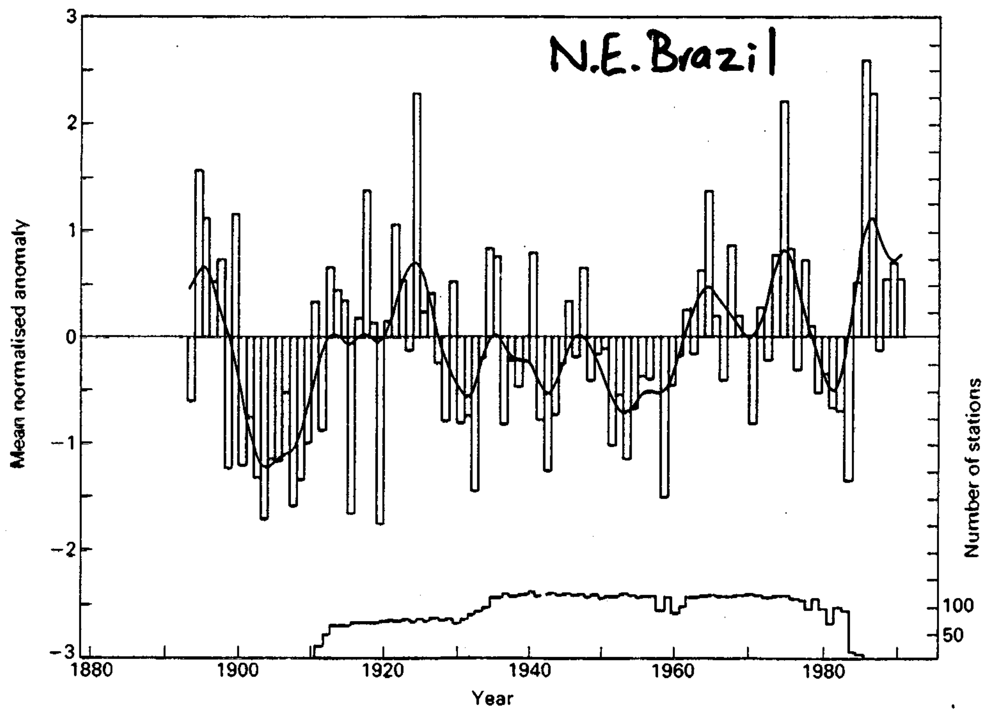

Figure 2 Time series of annual rainfall – Northeastern Brazil (1893–1990)

From UNEP Desertification Atlas

semi-arid regions pose a challenge to models

soil moisture

c.f. seasonal snow cover

- strong influence on fluxes
- large range of conditions over a year
- to model soil moisture reservoir over months needs accurate:

  evaporation
  deep drainage
  runoff

  also in a GCM need good forcing:

  rainfall
  solar radiation

This is DIFFICULT

I Diurnal Variability

flux observations

tiger bush (SSS) 20/8/92   HAPEX Sahel Southern Super Site

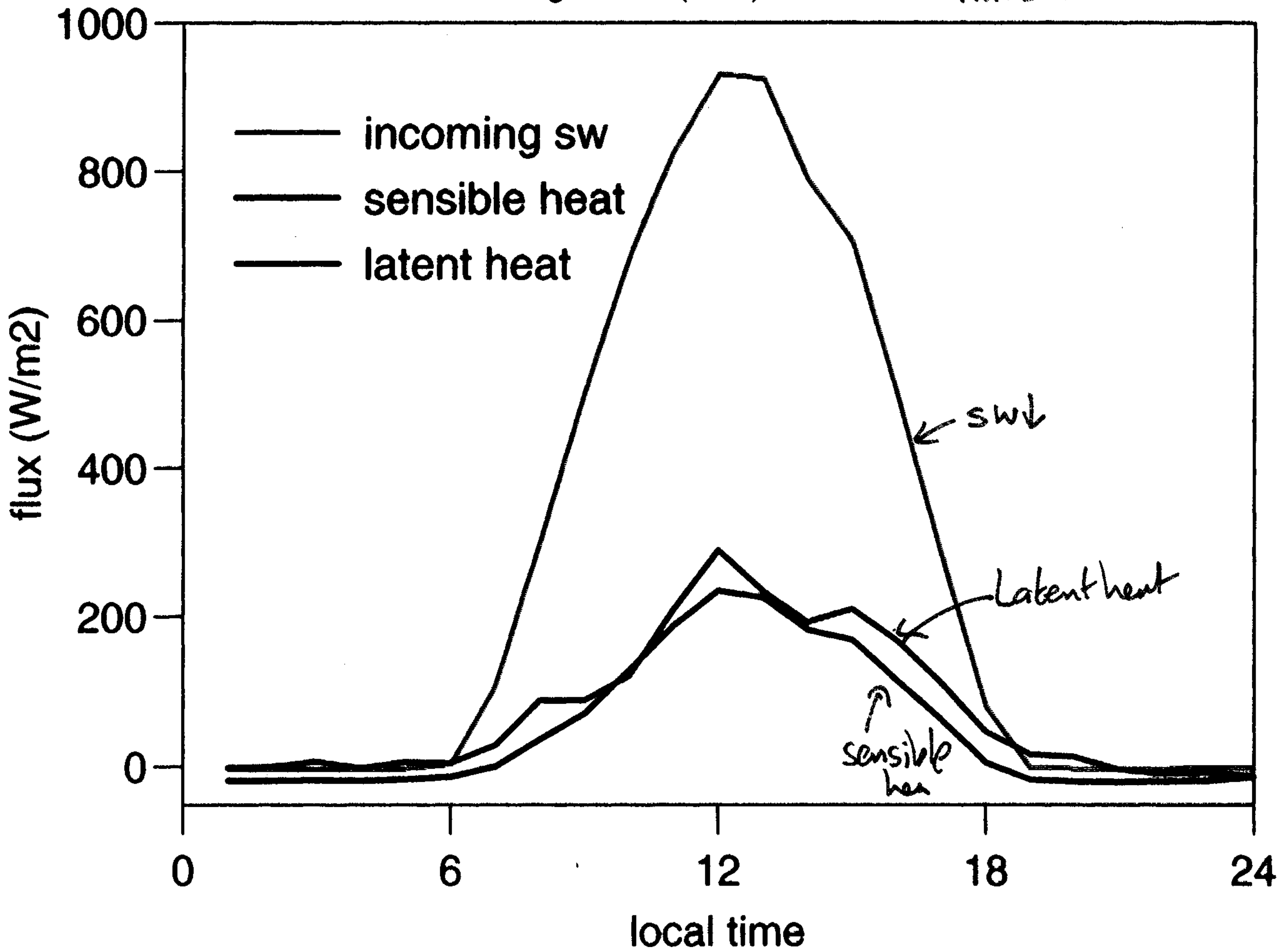

see Goutorbe et al for an overview of HAPEX-Sahel
or
HAPEX-Sahel special issue
Journal of Hydrology 188-189
1997

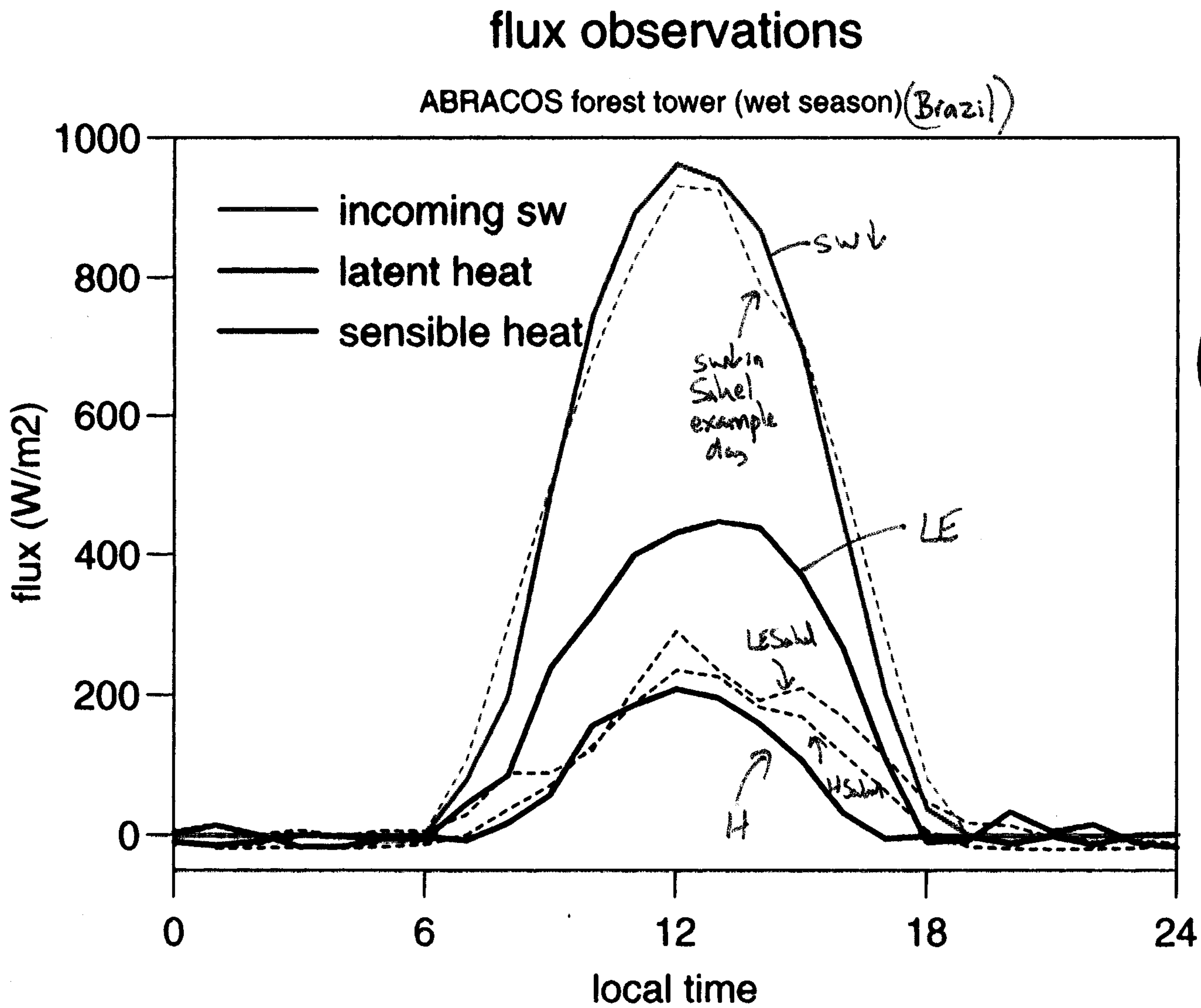

tropical forest
- higher available energy
$A = H + LE$
- often has higher evaporative fraction
$\frac{LE}{H+LE}$

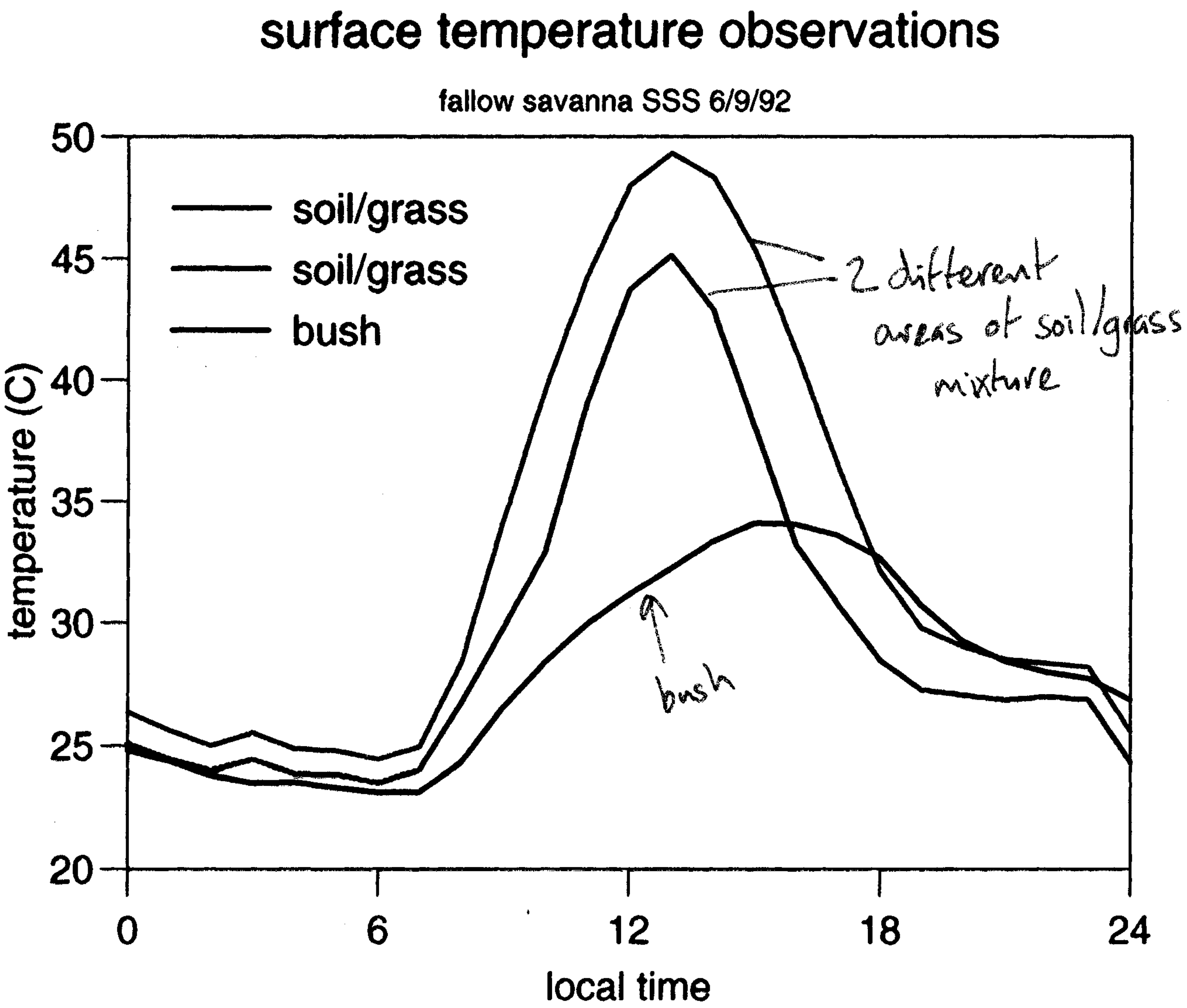
surface temperature observations
fallow savanna SSS 6/9/92
soil/grass
soil/grass
bush
temperature (C)
50
45
40
35
30
25
20
0
6
12
18
24
local time
2 different areas of soil/grass mixture
bush

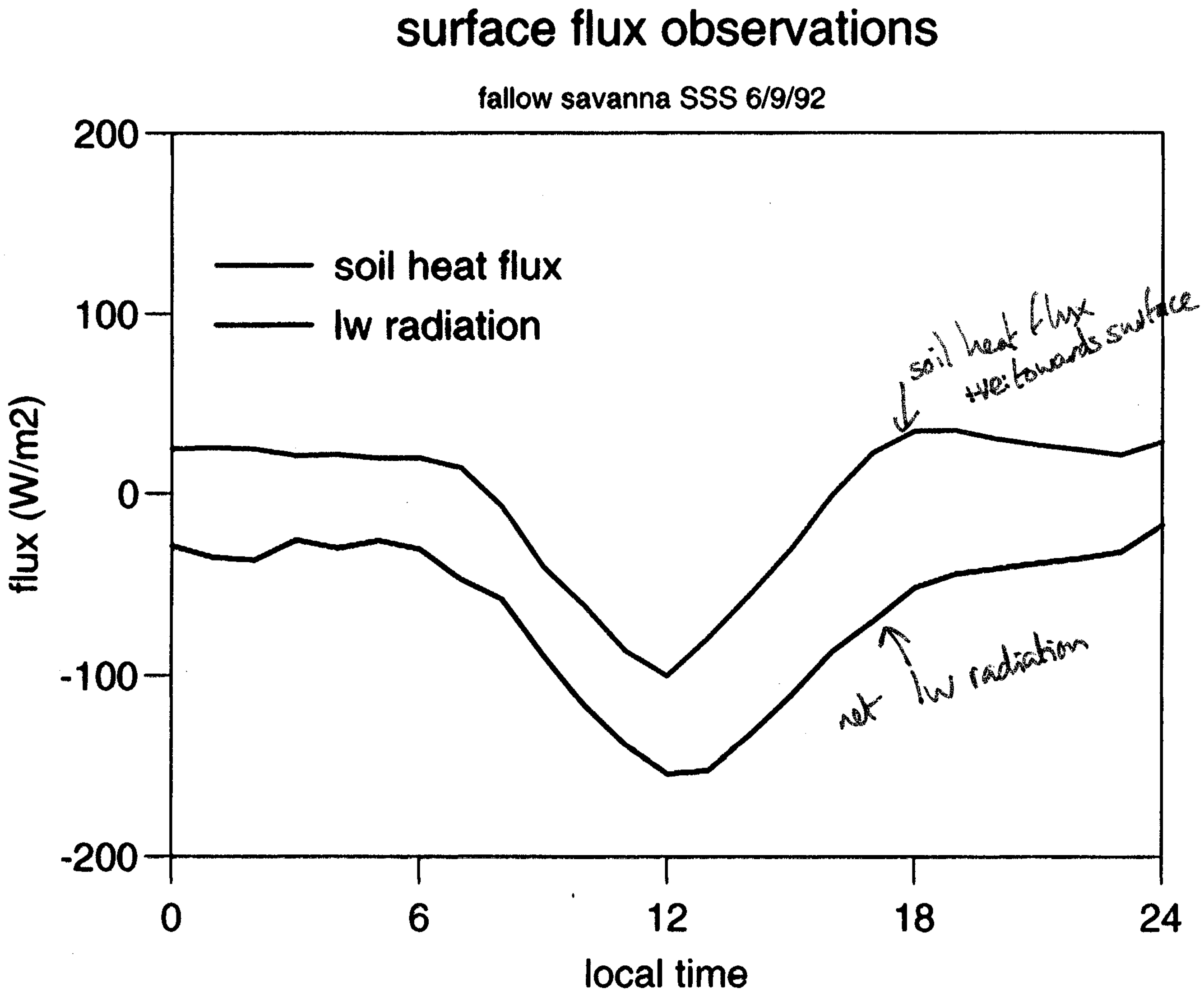
surface flux observations
fallow savanna SSS 6/9/92
soil heat flux
lw radiation
soil heat flux
+ve: towards surface
net lw radiation
200
100
0
-100
-200
flux (W/m2)
0
6
12
18
24
local time

Differences between sparse and dense vegetation

Sparse veg:

lot of exposed soil

∴ properties of soil have impact on surface fluxes

albedo*	~20-30%	c.f. tropical forest ~12%
ground heat* flux	can be 200 Wm^{-2} around midday	tropical forest negligible
long-wave* fluxes	dominated by hot soil (σT^4)	
evaporation		

* reduce available energy

1. Big Leaf Model →

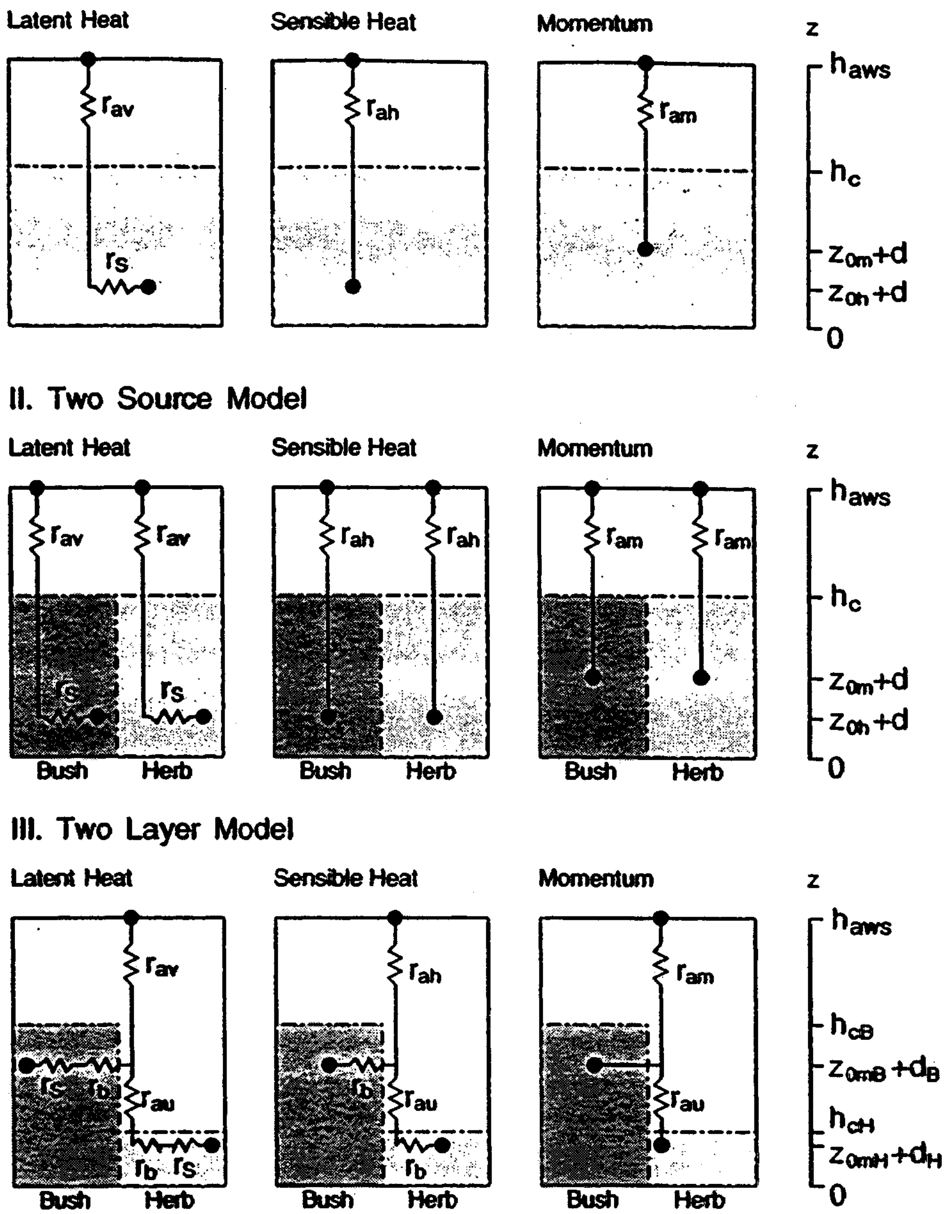

or bush/soil

Fig. 2. Schematic diagrams showing the resistance networks of the three models (height axis not to scale).

Penman-Monteith equation is assumed to hold for the bushes across aerodynamic resistance r_{b_B} and for the herbs across $r_{au} + r_{b_H}$ to a point $z = z_B$ with vapour pressure deficit D_B. λE is determined from (2) where

from Huntingford et al (1995)

$$\lambda E_B = \frac{\Delta A_B + \dfrac{\rho c_p D_B}{r_{b_B}}}{\Delta + \gamma\left(1 + \dfrac{r_{s_B}}{r_{b_B}}\right)}, \qquad (4)$$

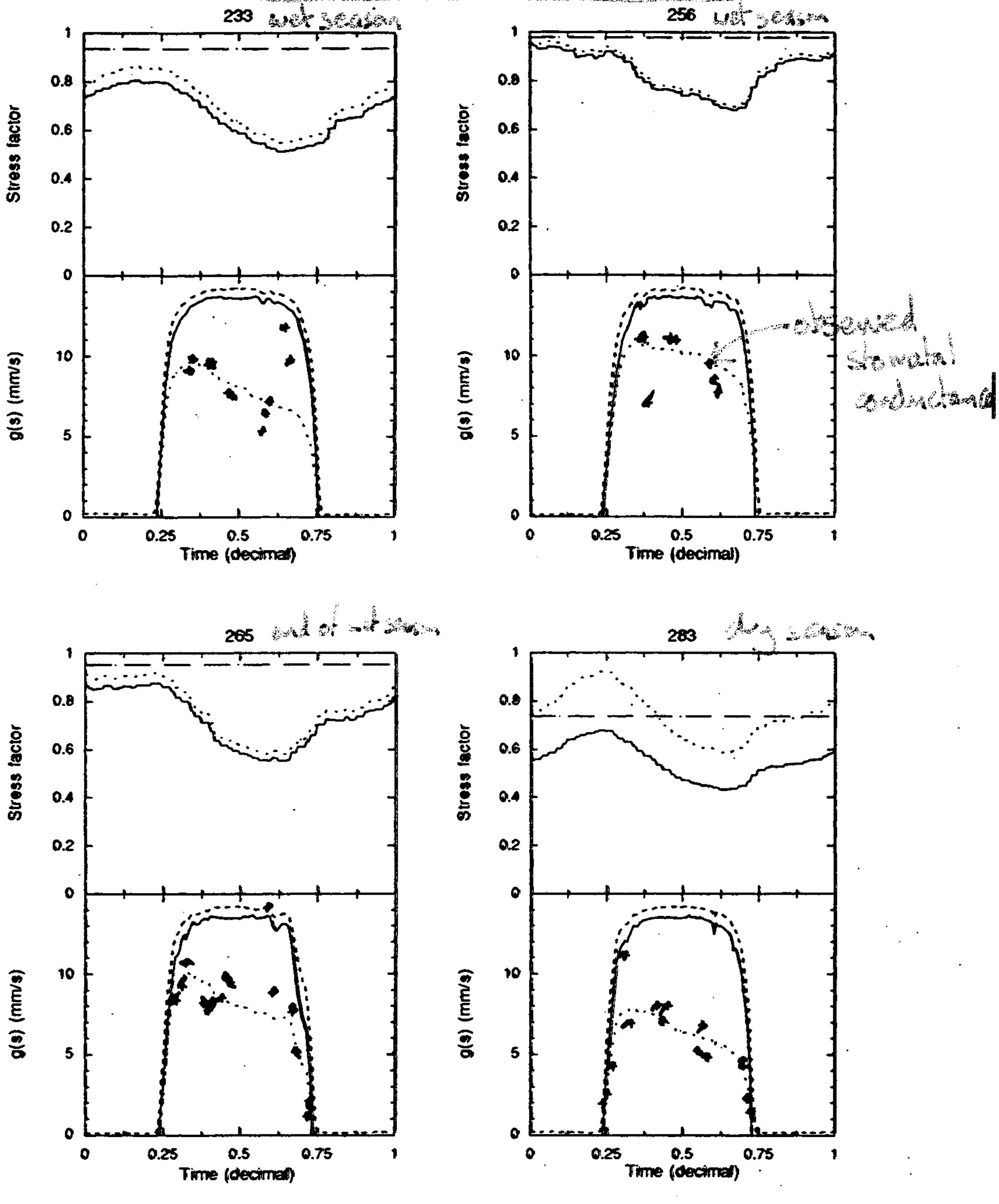

Fig. 5. Diurnal curves of environmental stress functions and the potential and actual stomatal conductances: (a) *Guiera senegalensis* (West-Central shrub fallow site), for selected days during the growing season of 1992.

stomatal conductance

plants control exchange of water and CO_2 with atmosphere by adjusting stomata according to environmental conditions

e.g.

$$g_s = g_{s\,max}\, f_1(\text{v.p.d.}) \times f_2(T) \times f_3(\text{P.A.R.}) \times f_4(\theta)$$

(P.A.R. = photosynthetically active radiation; θ = root zone soil moisture)

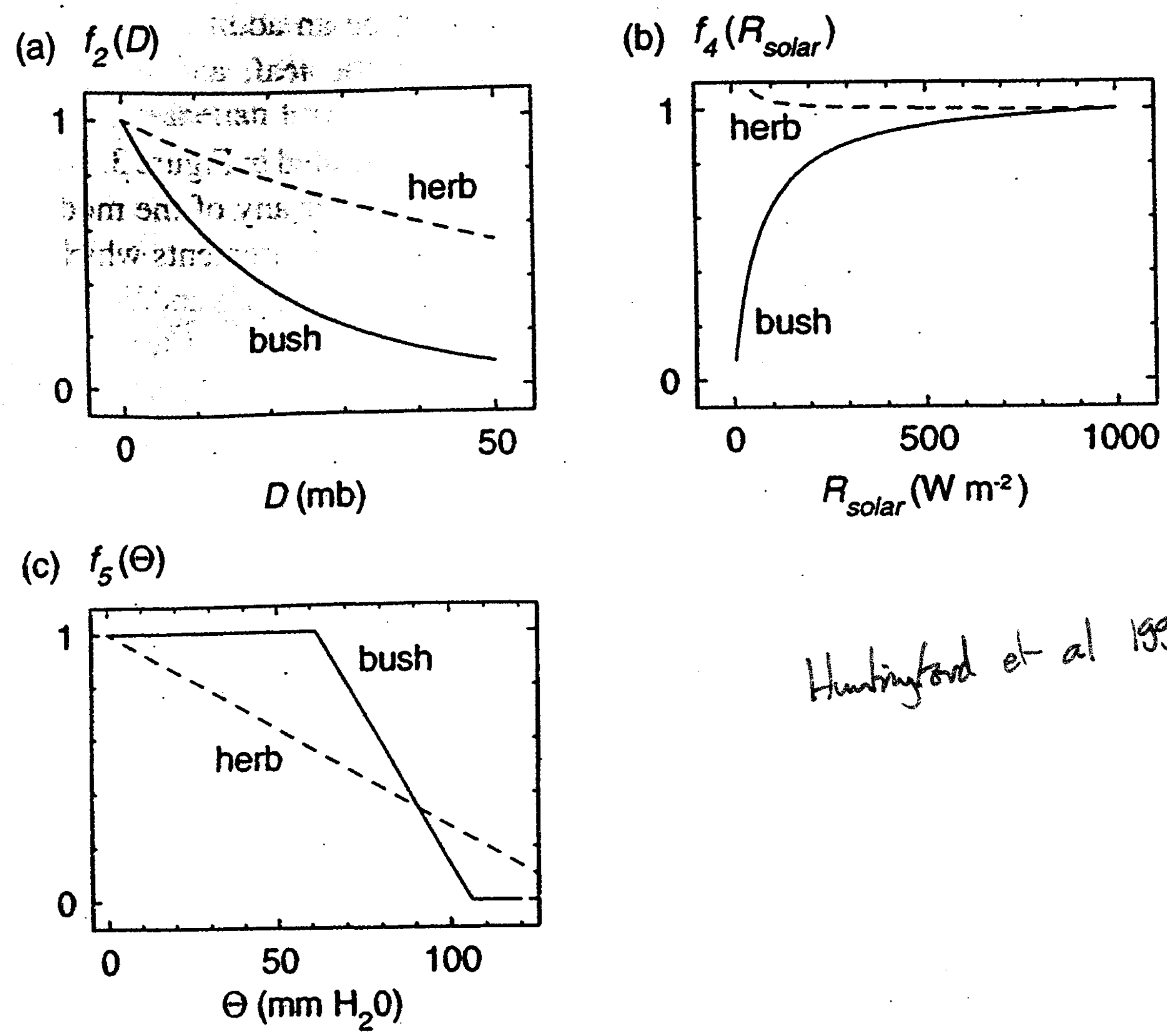

Huntingford et al 1995

Fig. 5. Stomatal response of bushes and herbs to (a) vapour pressure deficit, (b) solar radiation and (c) soil moisture deficit as determined using the Two Layer Model.

bush evaporation rate was optimized first, then the herb response a_{4_H} should be regarded as the optimization adjusting to compensate for a_{4_B} taking unexpected values.

Although it is recognised that the confidence limits on the a_4 values are large, the different values of a_{4_B} may be indicating something important about the aerodynamic resistance networks. Suppose r_{a_h} in the Penman-Monteith equation is artificially increased. To maintain a good fit of λE, the value of r_S must change too, but the amount by which it must adjust depends on the other variables in the equation. The variable with the highest variation is the available energy $R_n - G$ and it is found that the smaller the value this takes, the smaller r_S must be to compensate. As the available energy shows an almost identical diurnal trend to the incoming solar radiation, this provides an explanation why $a_{4_B} = -3.39$ for the Two Source Model, that is, the aerodynamic resistance for the bushes in the Two Source Model is too large...

For the Two Layer Model the opposite is happening. The value a_{4_B} is too high, which in turn is due to the resistance network for the bushes ...
issing resistance ...

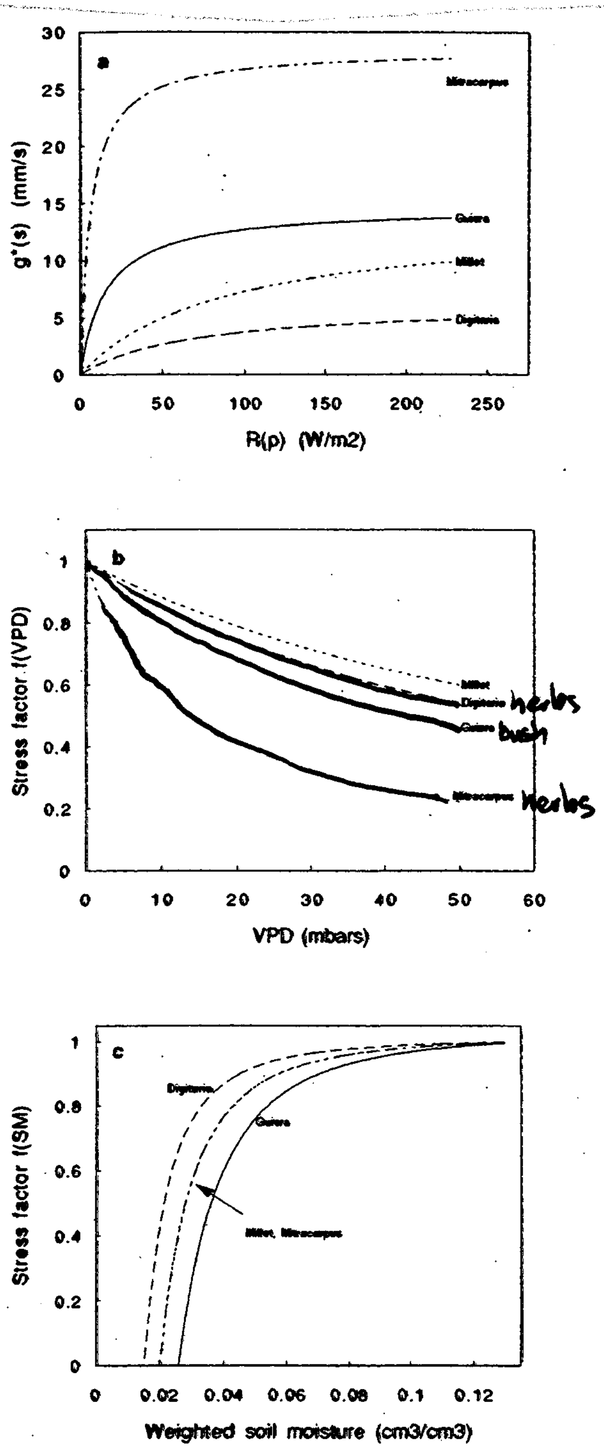
a
g*(s) (mm/s)
R(p) (W/m2)
Guiera
Millet
b
Stress factor f(VPD)
VPD (mbars)
herbs
bush
herbs
c
Stress factor f(SM)
Guiera
Weighted soil moisture (cm3/cm3)

stomatal conductance models

- optimisation procedures based on limited set of observations can give quite different results

- alternative to this approach is to base gs on (comparatively) well-vadidated models of leaf photosynthesis
  - → carbon fluxes
  - → shared dependencies of canopy conductance + p/s - fewer model parameters in principle

see e.g. Cox et al 1998

MOSES canopy conductance model

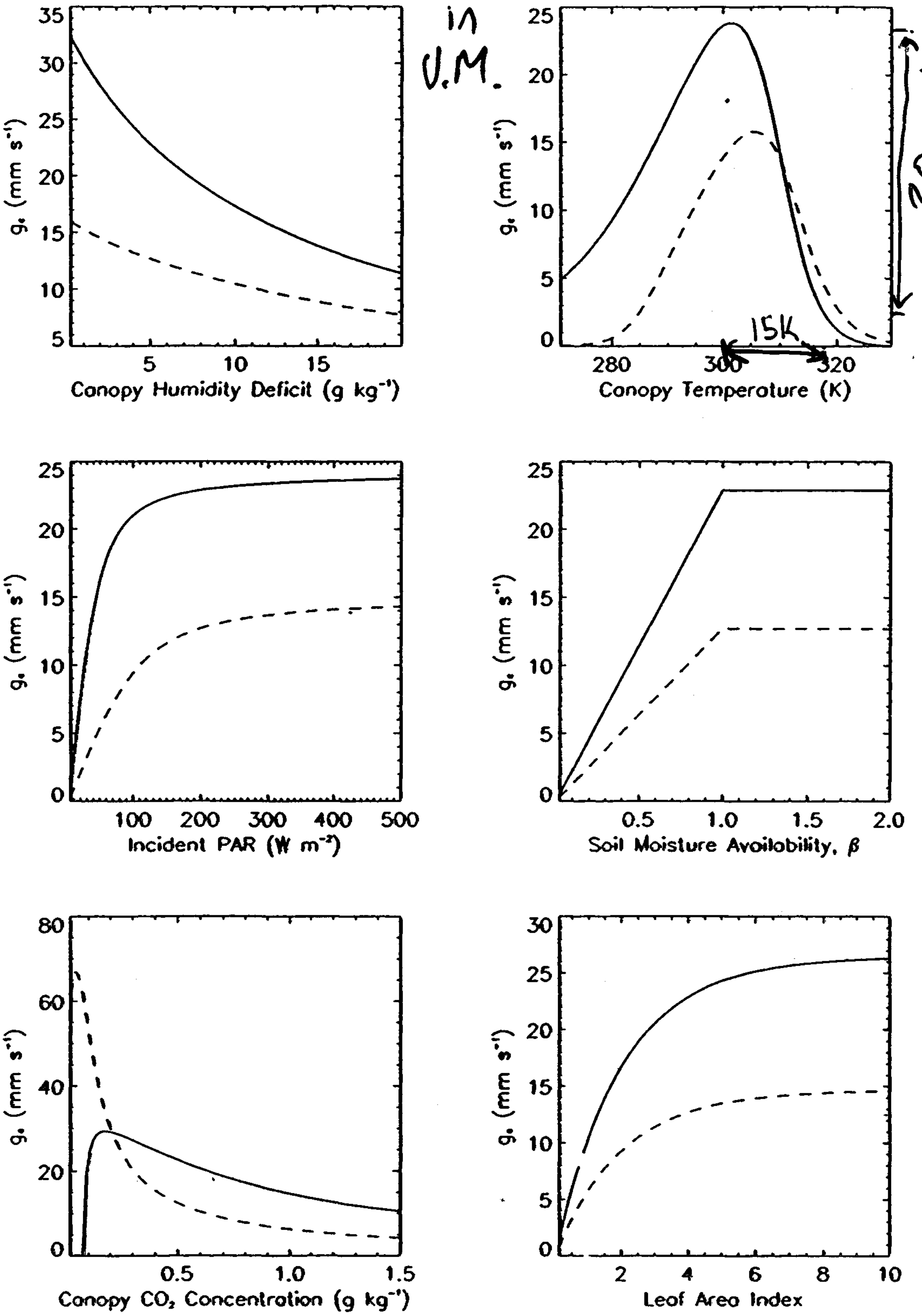

Figure 2: Dependences of the MOSES canopy conductance on environmental and structural variables. Typical responses of C_3 and C_4 grasses are represented by the continuous and dotted lines respectively. (Defaults : $dq = 5.0\,g\,kg^{-1}$, $T = 298.15$ K, $\beta = 1.0$, $PAR = 200$ W m^{-2}, CO_2=0.490 g kg^{-1}, LAI=4.0).

description of MOSES - Cox et al 1999

in practice, conductance/photosynthesis models can show unrealistic behaviour when coupled to imperfect GCMs

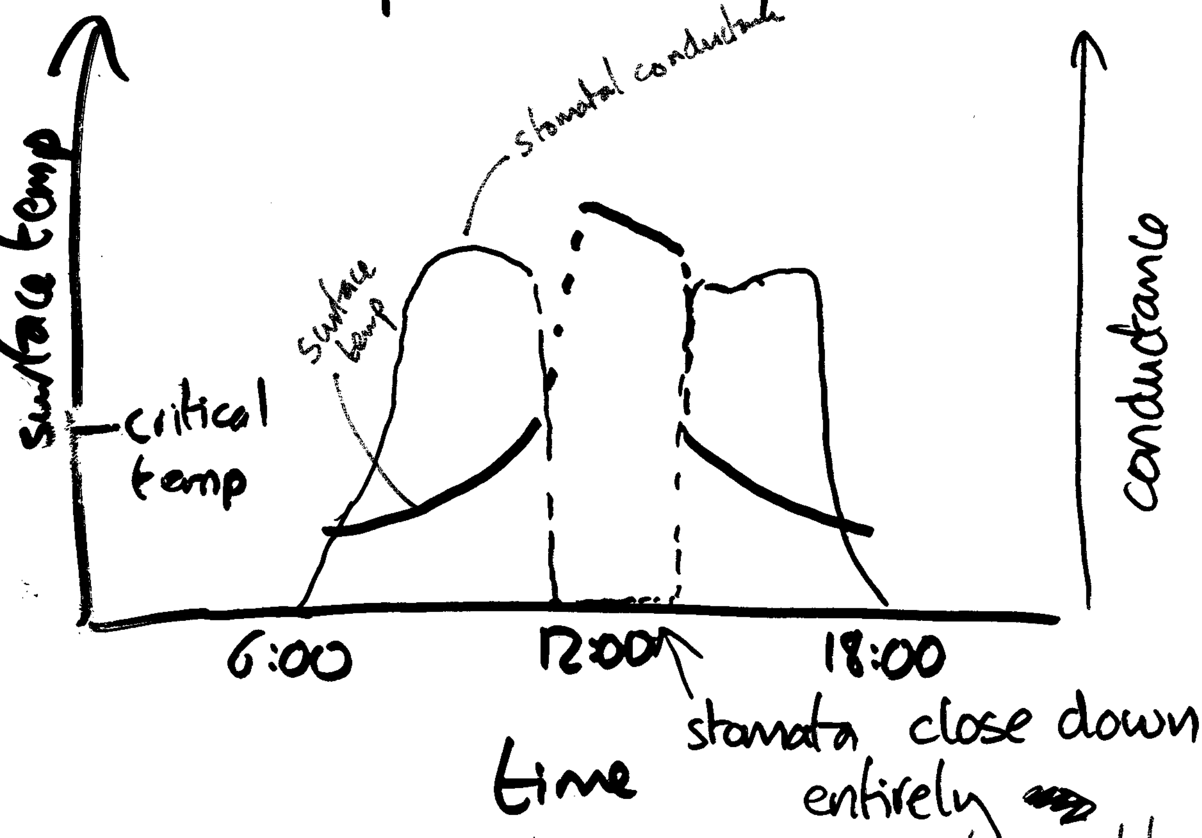

possible behaviour in complex model of conductance + photosynthesis coupled to imperfect GCM

II daily variability

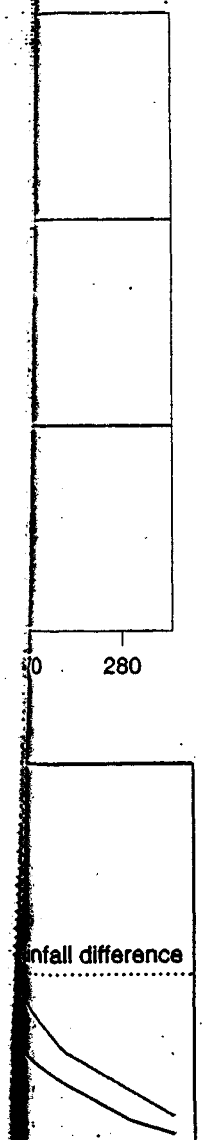

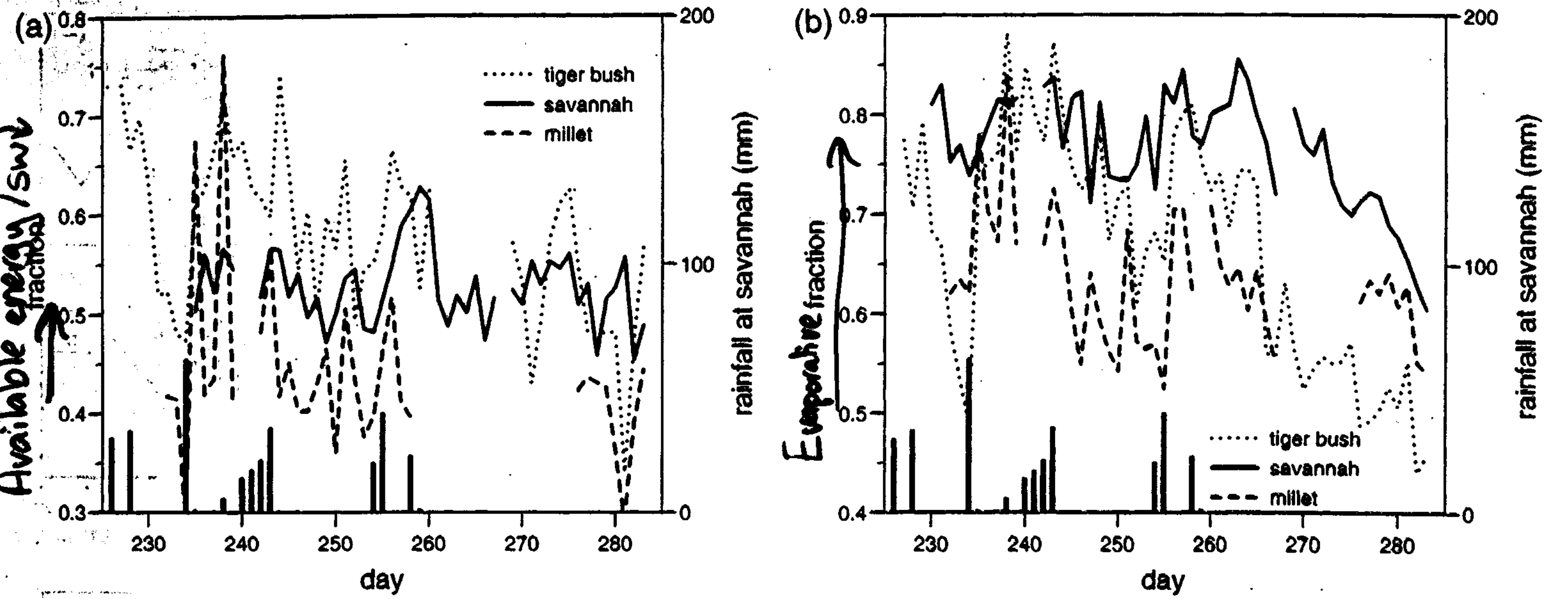

FIG. 5. Daytime averaged values of (a) available energy normalized by incoming shortwave flux and (b) evaporative fraction for the three SSS subsites. The daily rainfall (mm) at the savannah site is also shown.

II daily variability

Soil moisture evolution after rainfall

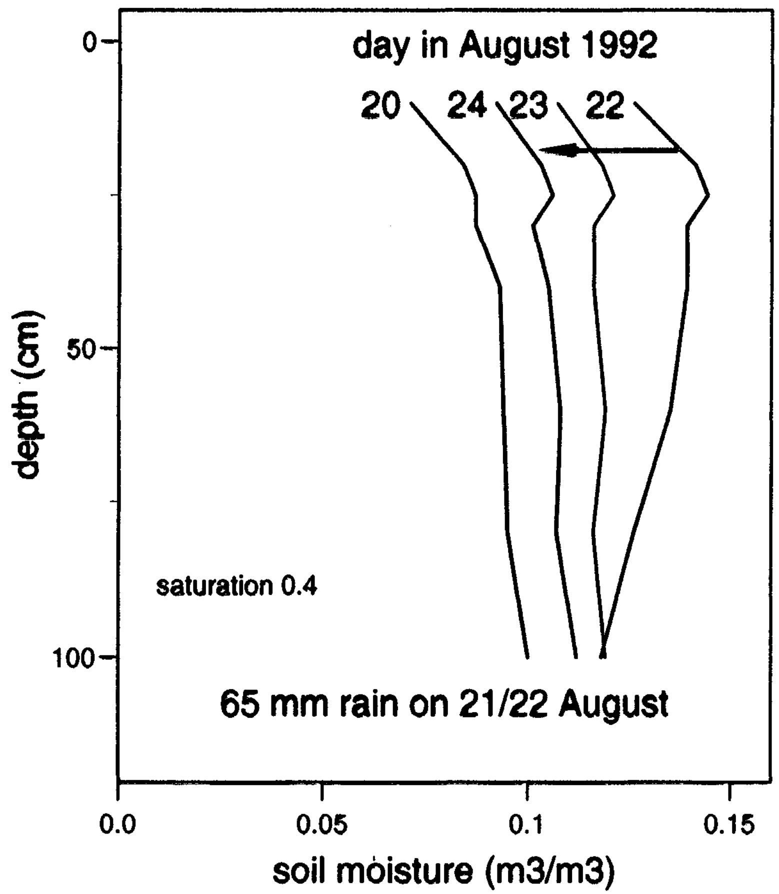

Direct evaporation from bare soil can exceed 3 mm/day (100 W m^{-2}) for 1-2 days after rain

During wet season, rain events generate variability in LE and H

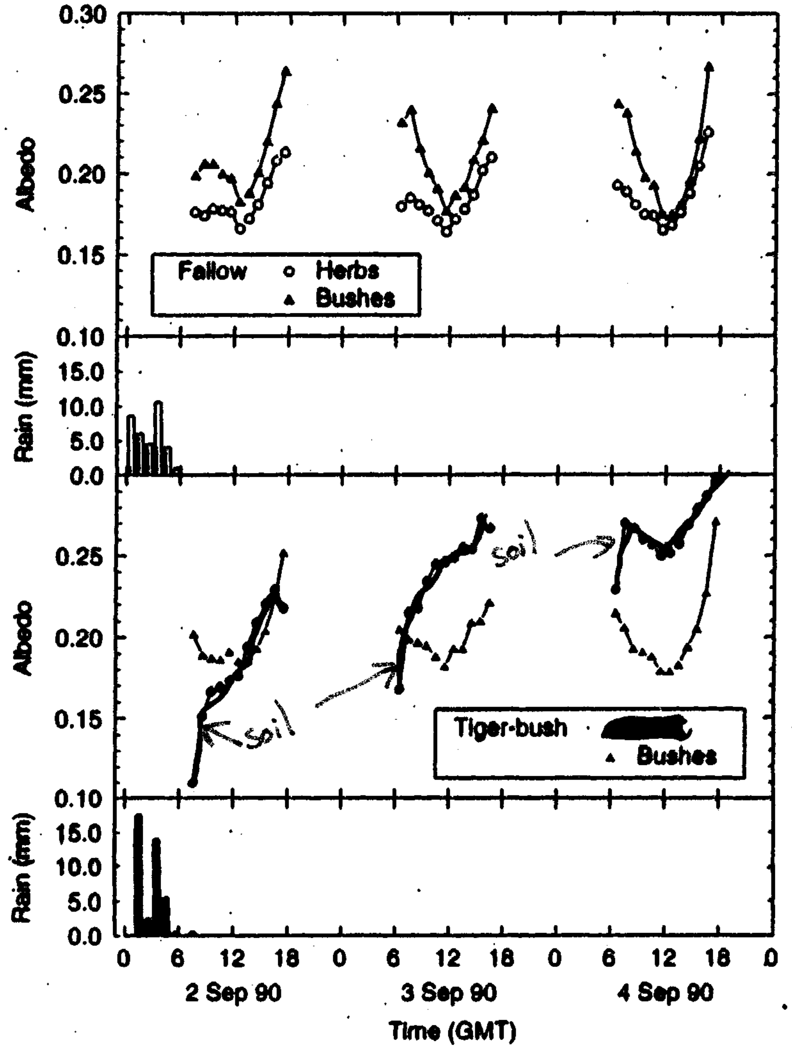

Figure 2. Variation in hourly mean albedo for the component surfaces at the fallow and tiger-bush sites over a 3-day period following a rainstorm (hourly rainfall totals also shown).

from Allen et al 1994

modelling soil moisture movement

Darcy equation

$$W = K \left\{ \frac{\partial \psi}{\partial z} + 1 \right\}$$

K hydraulic conductivity

ψ soil water suction

both K and ψ depend on θ and properties of soil

eg

$$K = K_{sat} \left(\frac{\theta}{\theta_{sat}} \right)^{2b+3}$$

$$\psi = \psi_{sat} \left(\frac{\theta}{\theta_{sat}} \right)^{-b}$$

↳ θ_{sat}, K_{sat}, ψ_{sat} and b all need to be specified for every soil type levels

sensitivity of water fluxes to specification of hydraulic parameters

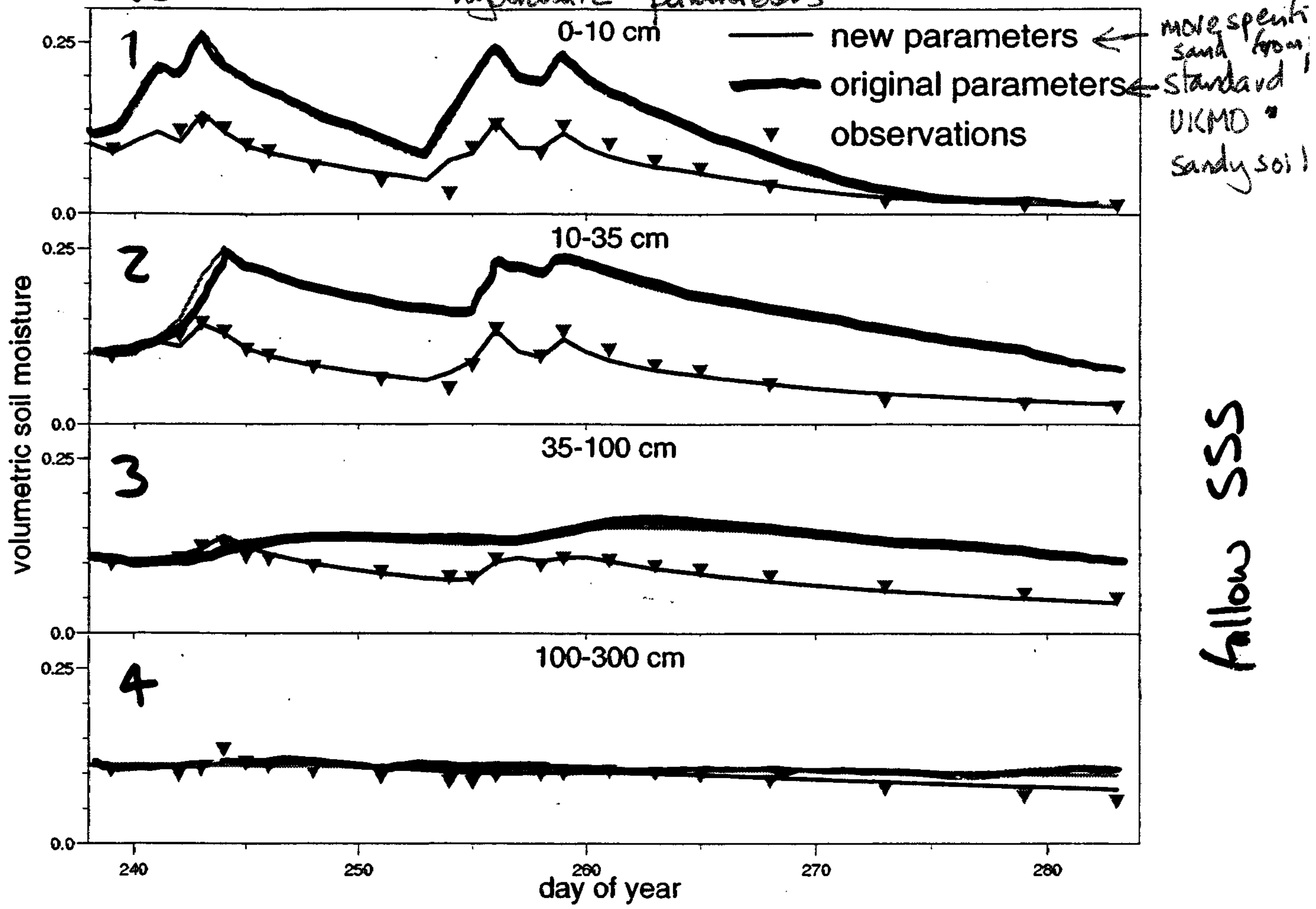

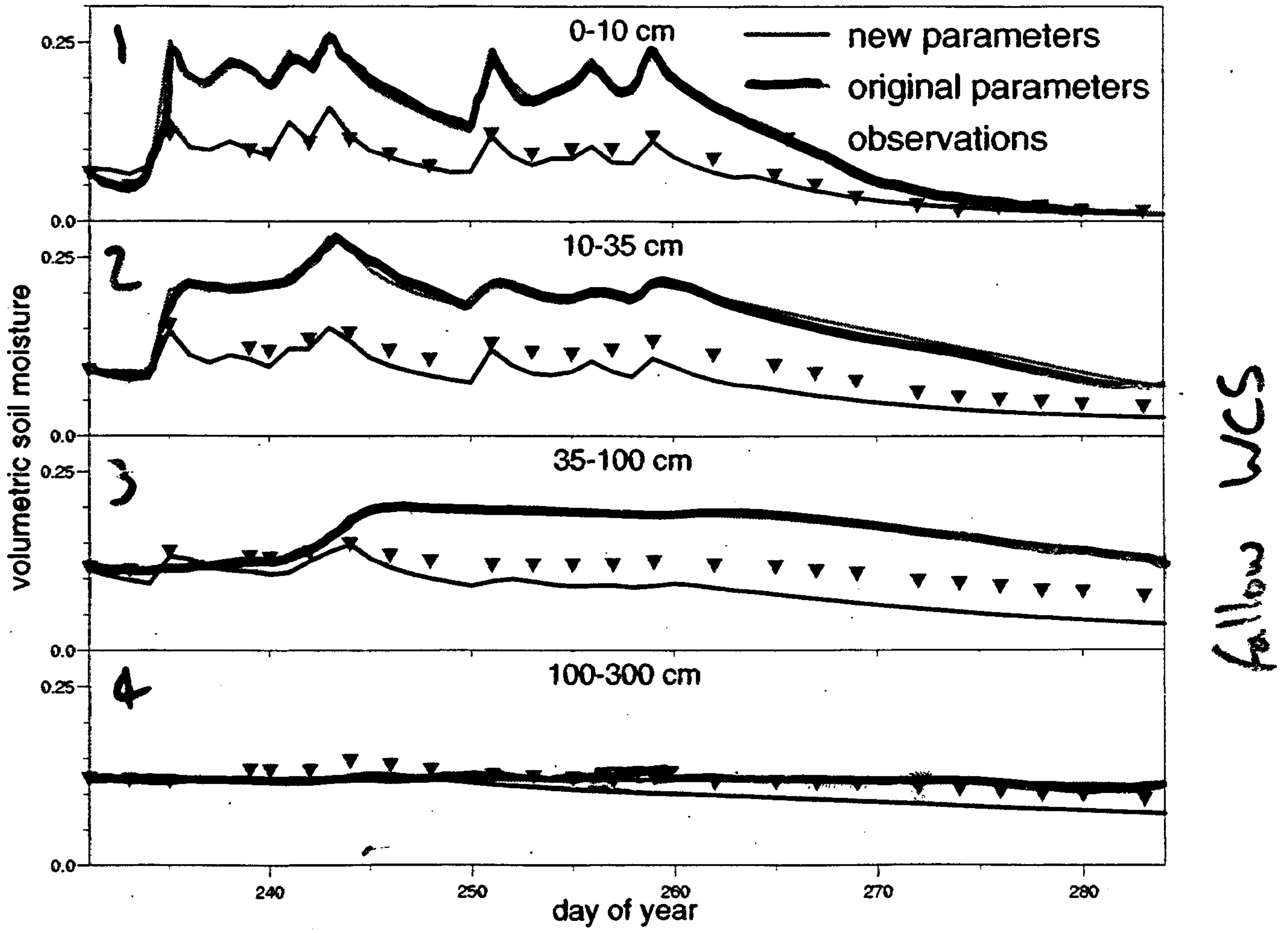

3	$E_g = \frac{\rho}{R_a}\beta[q_{sat}(T_s) - q_a]$	with β
4	$E_g = \frac{\rho}{R_a + R_{soil}}[hq_{sat}(T_s) - q_a]$	with R
5	$E_g = \min\left\{\rho_w E_t, \frac{\rho}{R_a}[q_{sat}(T_s) - q_a]\right\}$	with E

the maximum values being for a comparable value of soil moisture ($w_g \approx 0.60 w_{sat}$). Figure 4b shows that $\beta = \alpha$ from NP89 fits this set of curves quite well.

Test 4 corresponds to the more complex β method used by Dorman a
to test 2 except f
potential in Eq. (
Hornberger (1978
silty clay loam (ψ
= 7.75).

Test 5 correspo
mulation. In Fig.
[Eqs. (MP84), (D
face moisture con
= 0.3 m^3 m^{-3} whi
of the curves beh
than 100 W m^{-2}
formulation of Al
has very high valu
will first occur at a
moisture. Since E
moisture, this me
evaporation form
to the other ones.
The formulation o
chosen because it i
ple two-layer moc
to Eq. (9) from W
set to $2d_1/C_1$ as
(1989). This lead

We first examin
surface water cont
and the cumulati
seven experiment

Six experiment
content obtained a
6a. These measur
dient of water in
formation of a su
for details). The p
w_g during the firs
quasi-steady beha
(except for test 5)
oration is compen

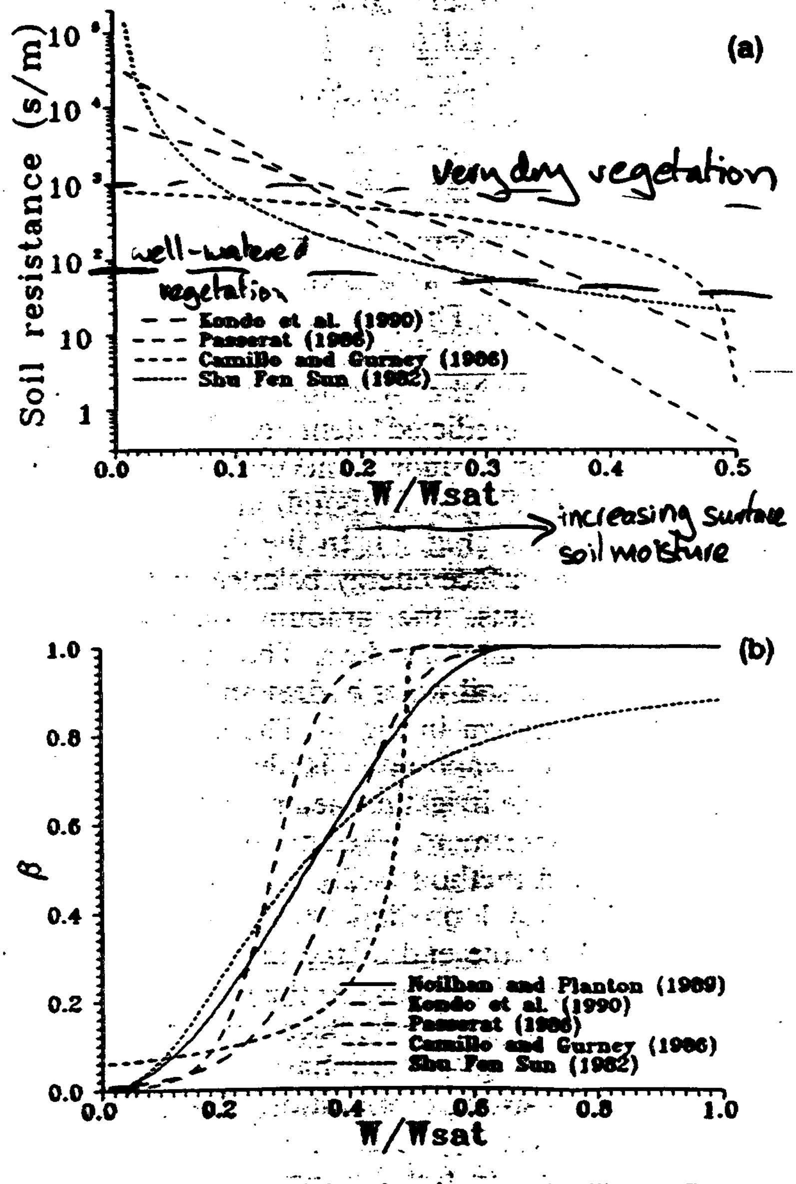

FIG. 4. Soil resistance (a) and moisture availability coefficient β (b) as function of relative water content (see Table 1). The coefficient β is computed for a value of R_a = 50 s m^{-1}.

from Mahfouf + Noilhan 1991

III seasonal variability

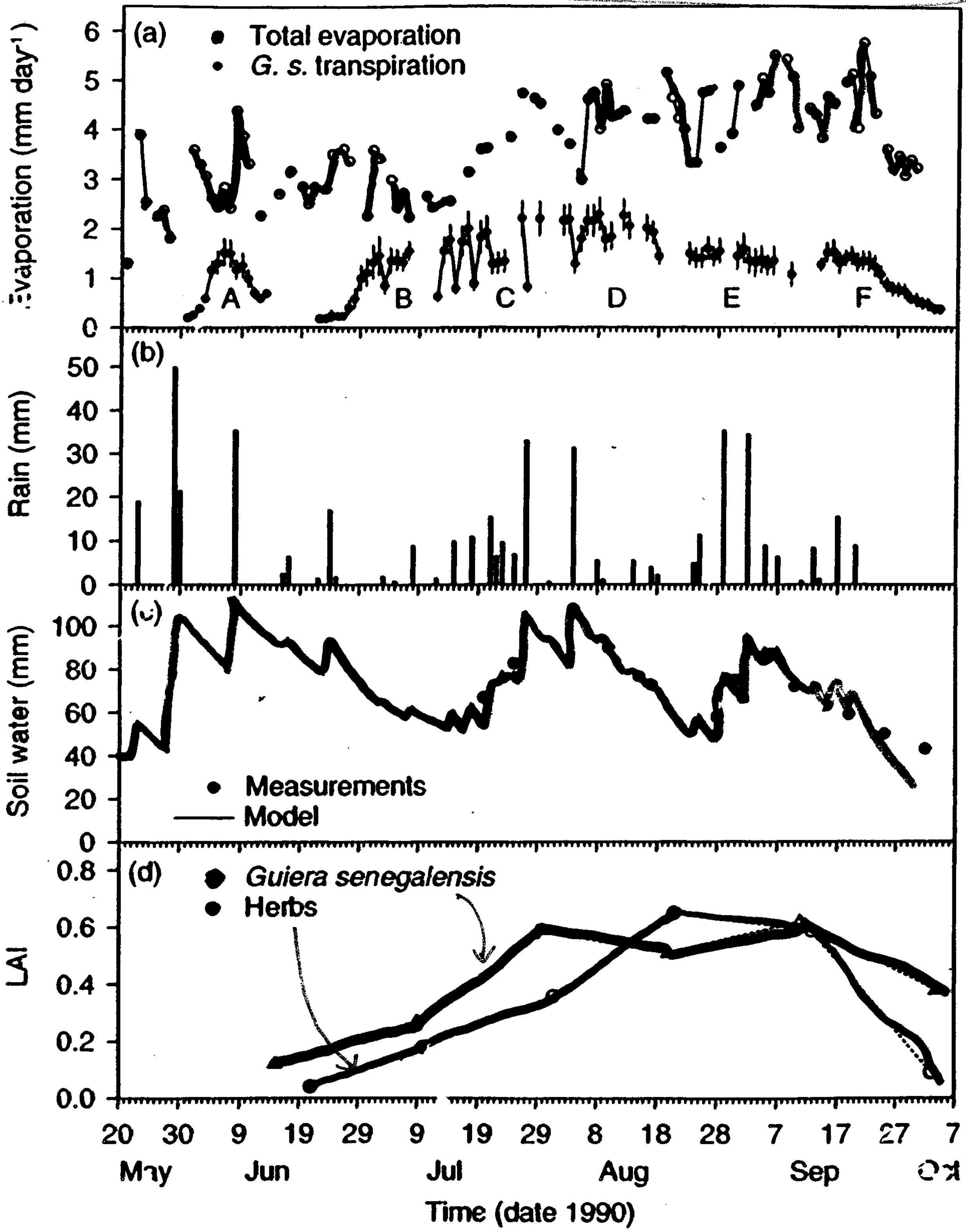

Components of the fallow savannah water balance and leaf area growth over the 1990 wet season: tal evaporation (measured by eddy correlation) and daily total *G. senegalensis* transpirat ed by sap flow gauges, mean ± SE); (b) daily rainfall; (c) measured and modelled soil pro ontent; (d) leaf area indices of *G. senegalensis* and herbaceous understorey.

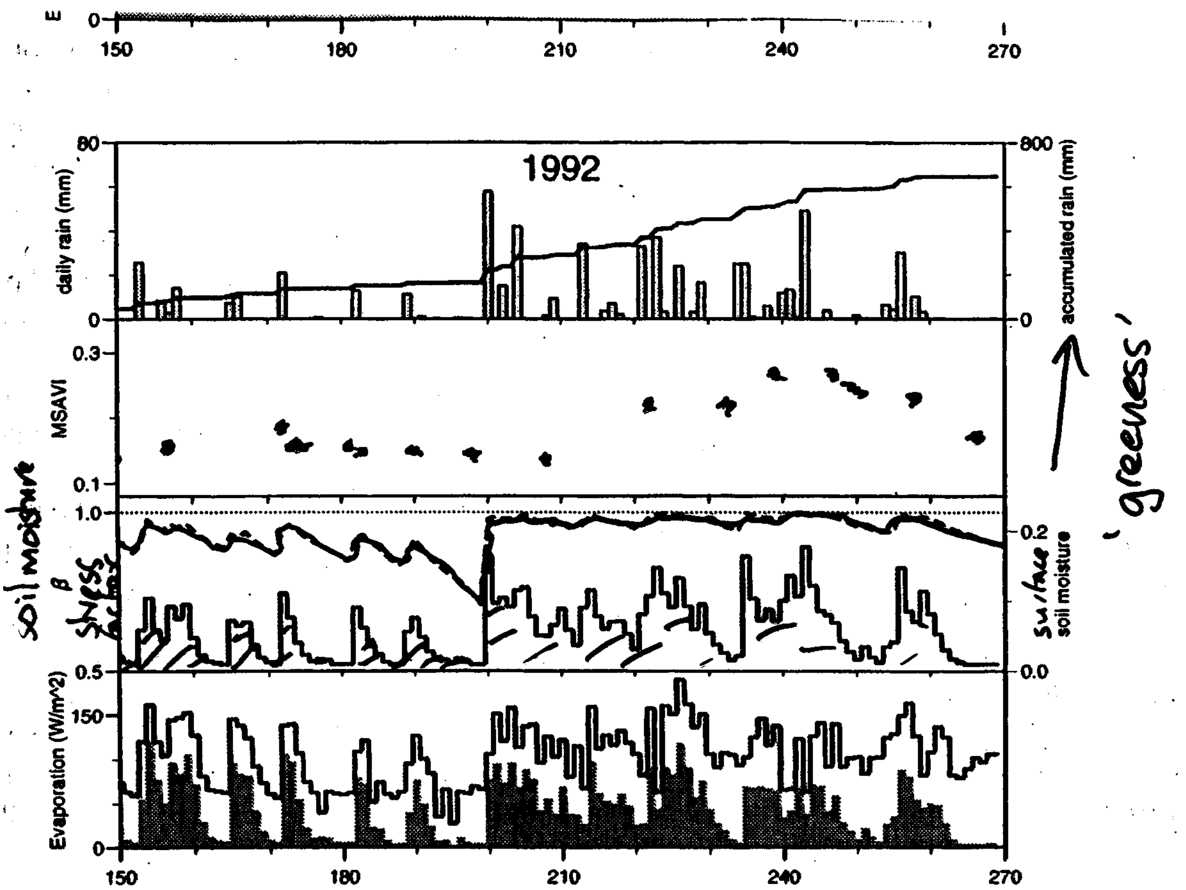

Figure 3. Summary of conditions averaged over the SSS stations for (a) 1991 and (b) 1992. Top panel: daily (bars) and accumulated rainfall. Second panel: MSAVI. Third panel: modelled soil moisture stress function (β) for fallow savannah (dashed) and 0–5 cm volumetric soil moisture ($m^3\ m^{-3}$; solid). Bottom panel: modelled daily total evaporation (line) and contribution from bare soil (shaded)

Taylor 2000

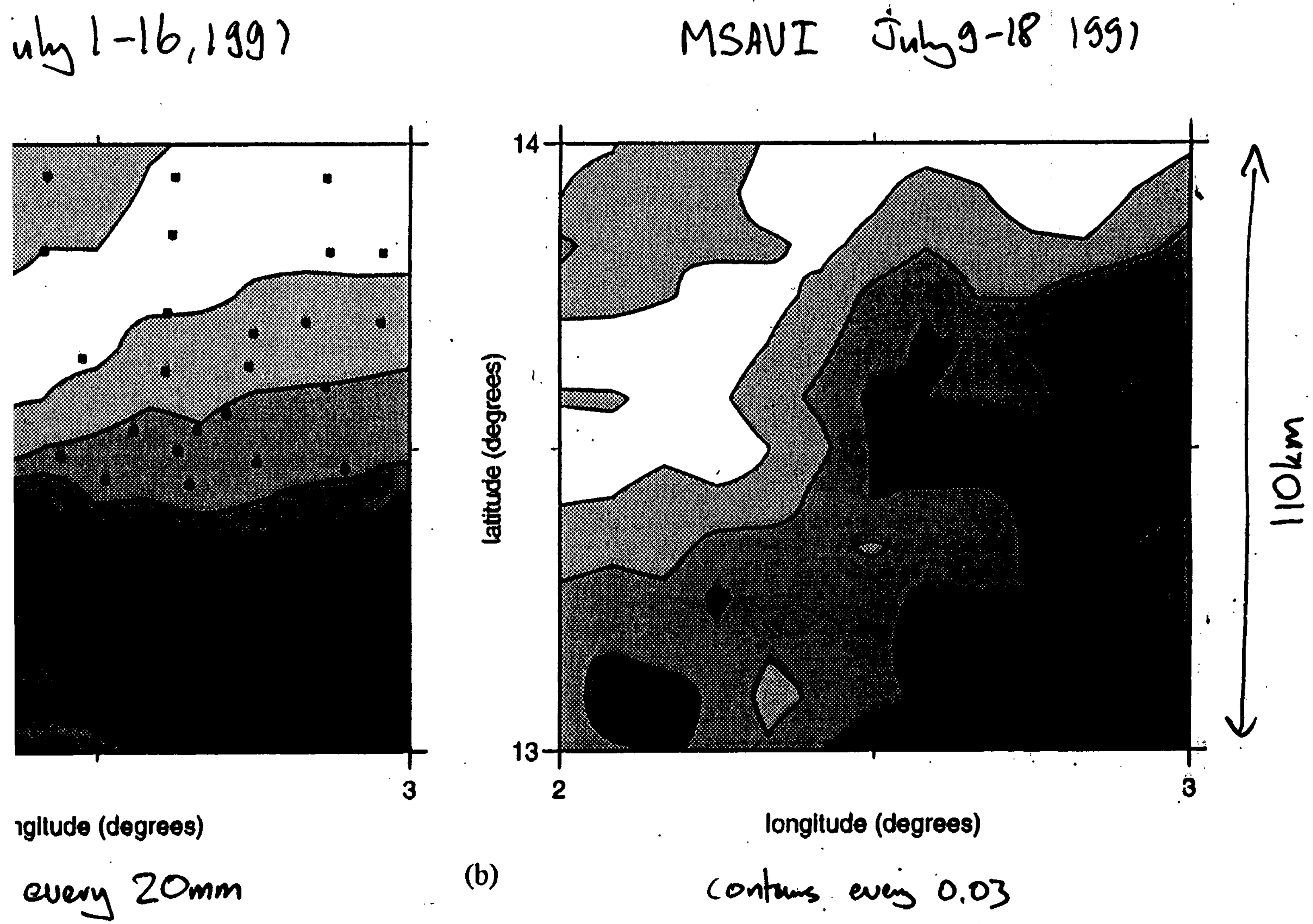

(b)

impact of rainfall on leaf area

Taylor + Blyth JGRd 2000

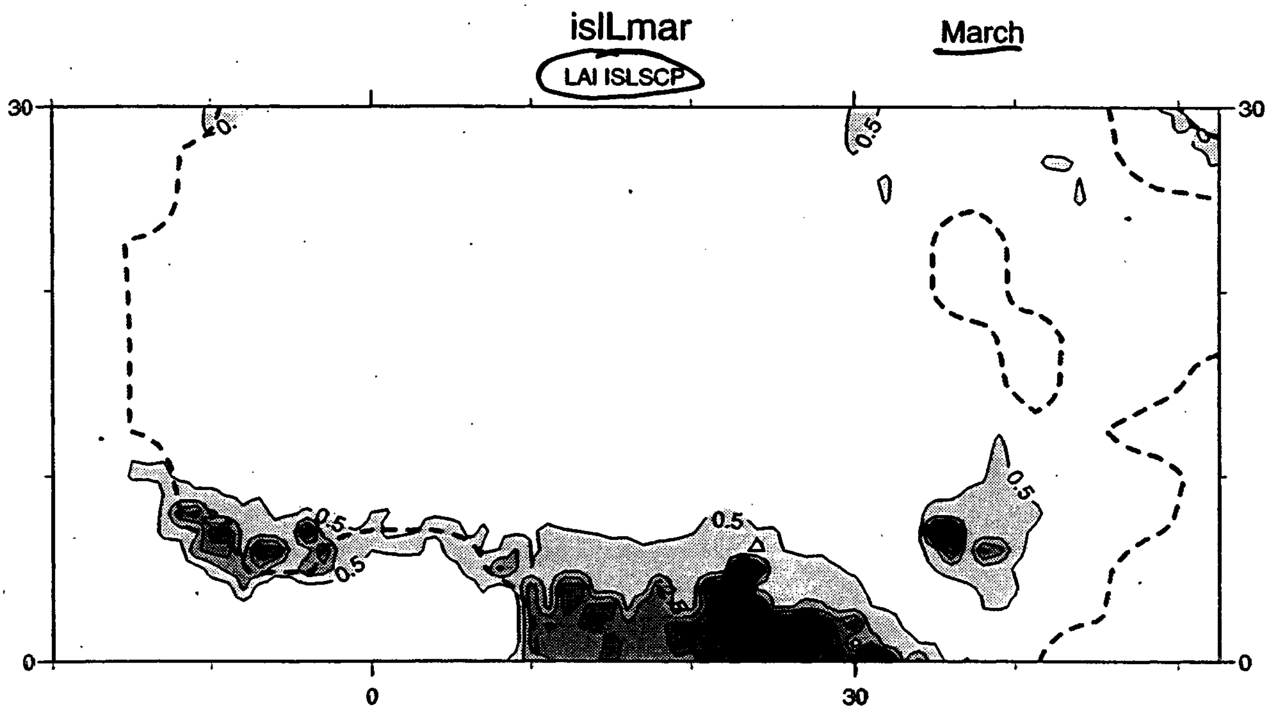

ISLSCP I LAI data
over ~~West~~ North Africa

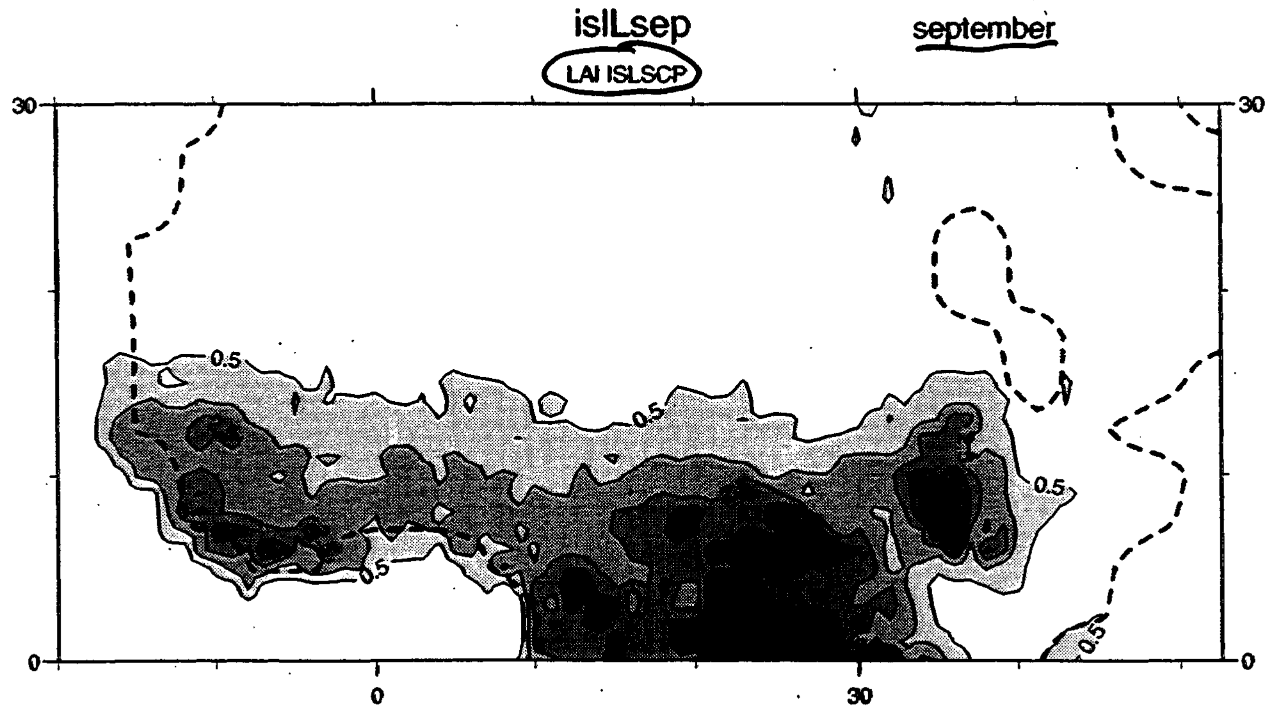

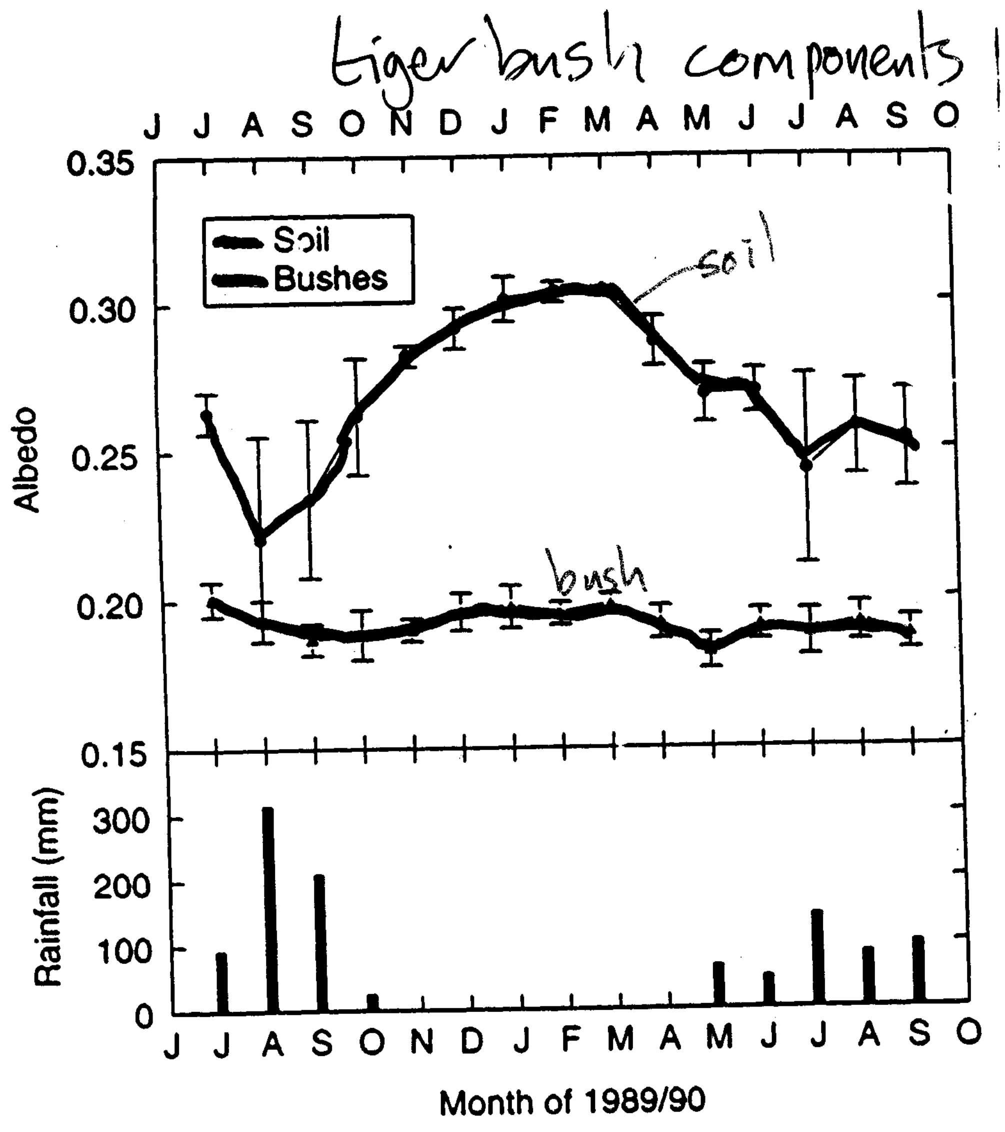
tiger bush components
Soil
Bushes
soil
bush
Albedo
0.35
0.30
0.25
0.20
0.15
Rainfall (mm)
300
200
100
0
J J A S O N D J F M A M J J A S O
Month of 1989/90

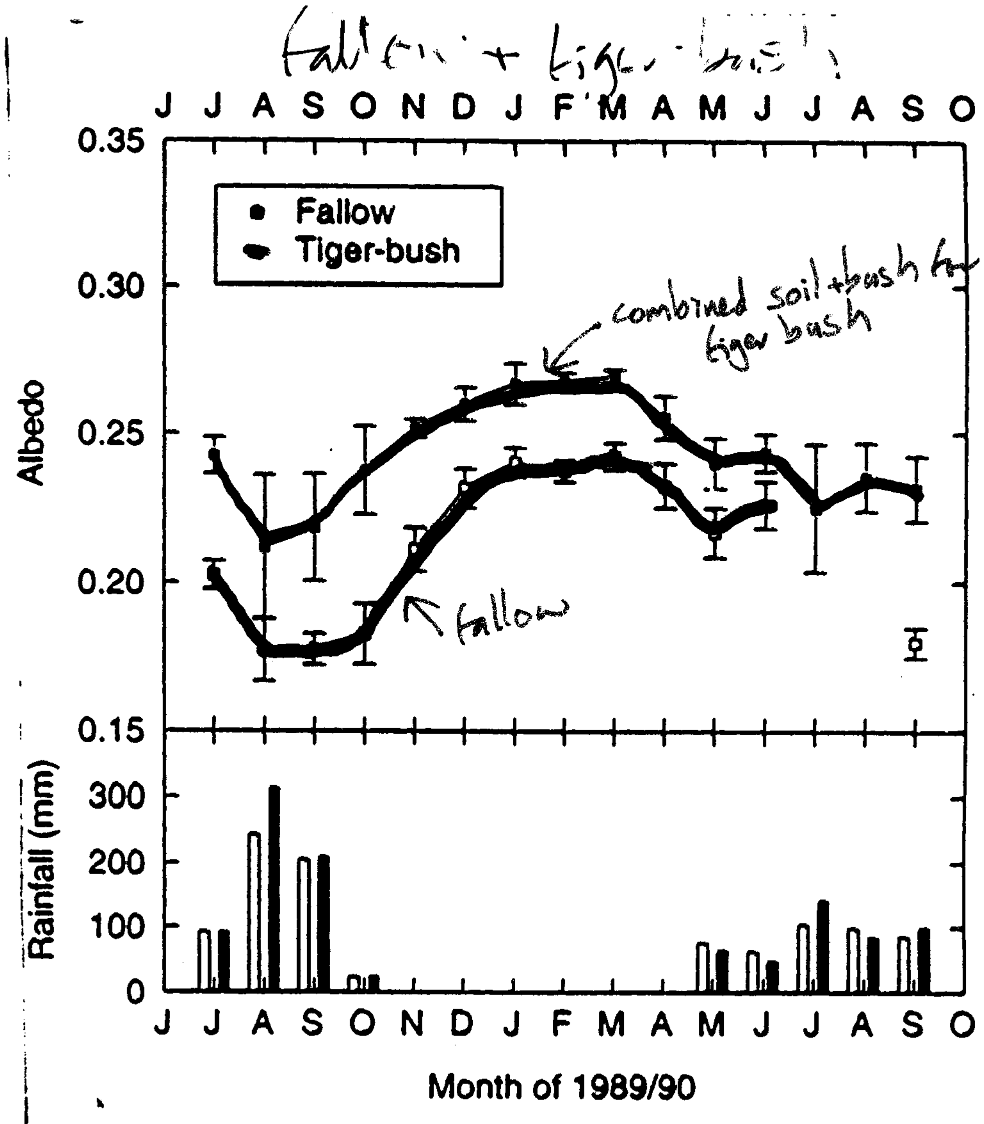
Fallow
Tiger-bush
combined soil+bush for tiger bush
fallow
Albedo
0.35
0.30
0.25
0.20
0.15
Rainfall (mm)
300
200
100
0
J J A S O N D J F M A M J J A S O
Month of 1989/90

Allen et al

Gaze et al

dry season soil moisture measurements in savanna

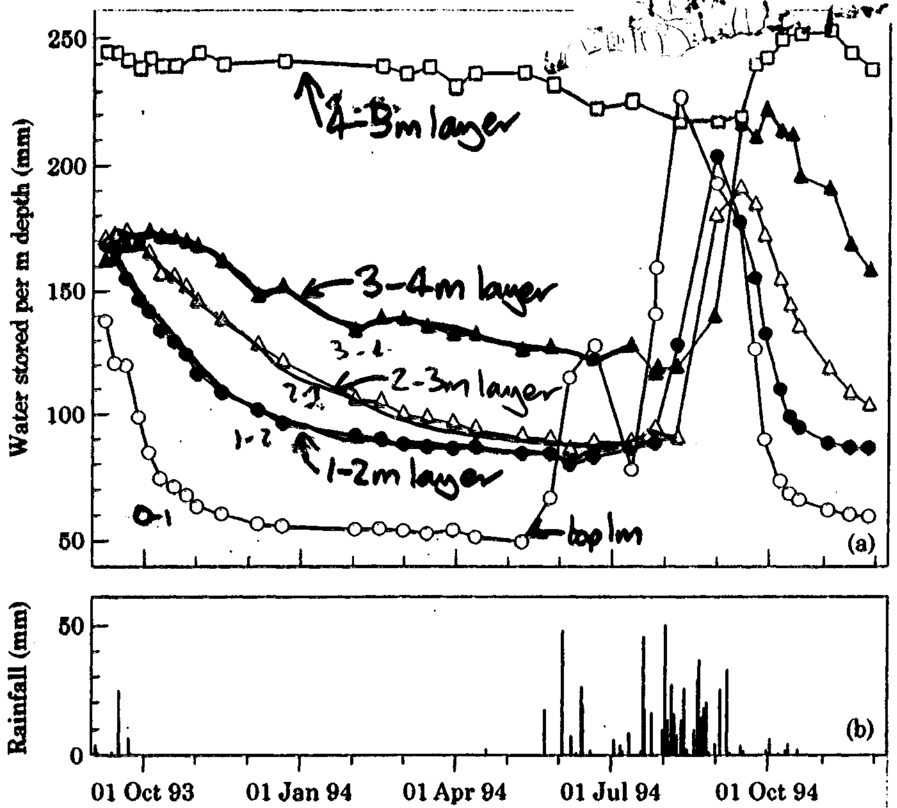

Figure 3. (a) Mean soil water storage for depth increments of 0–1 m (○), 1–2 m (●), 2–3 m (△), 3–4 m (▲) and 4–5 m (□), and (b) daily rainfall between September 1993 and November 1994 at a *Guiera senegalensis* savanna in south-west Niger.

1993. It might therefore reasonably be assumed that the drying of the soil profile in the [illegible] solely to evaporation from the soil surface and plant oad, Girton,

Gaze et al

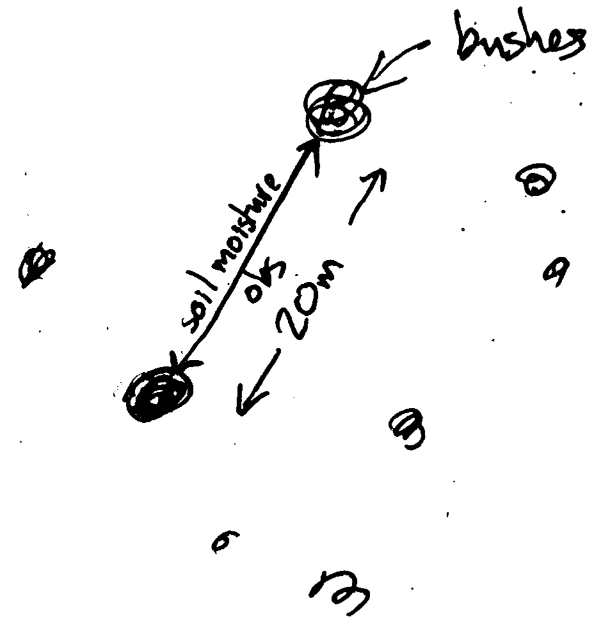

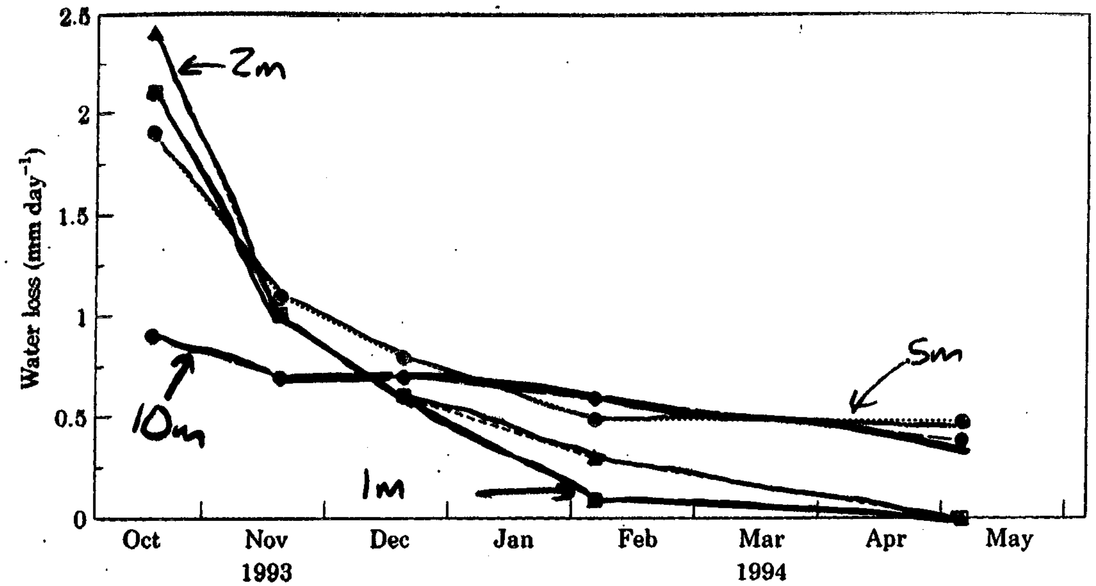

Figure 4. Temporal patterns of water loss during the dry season at different distances from the nearest *Guiera senegalensis* bush in a savanna in south-west Niger: (□) = 1 m; (△) = 2 m; (○) = 5 m; (●) = 10 m.

5404 was 151 mm, equivalent to 28% of the 1993 annual rainfall. Of this water loss, 59% (89 mm) was from depths greater than 2 m. In the absence of the deep-rooted *G. senegalensis*, this water would otherwise have contributed to ground-water recharge below the site.

IV Interannual Variability

Zeng et al

...ysics and Planetary Physics, University of Cal...
Los Angeles, CA 90095–156... USA. [2]NASA-
...d Space Flight Center, Greenb... , MD, 20771,

...hom correspondence should be addressed. E-
...eng@atmos.ucla.edu

was modified to account for the effects of leaf-to-canopy scaling (*20*) so that the canopy conductance g_c for evapotranspiration is

$$g_c = g_{s\max}\beta(w)(1 - e^{-kL})/k \qquad (2)$$

...Annual rainfall anom-
...rtical bars) over the
...African Sahel (13N-
...5W-20E) from 1950
...8. (A) Observations
...Hulme (*1*), (B) Model
...noninteractive land
... hydrology (fixed soil
...re) and noninterac-
...getation (SST influ-
...nly, AO). Smoothed
... a 9-year running
...howing the low-fre-
... variation, (C) Model
...teractive soil mois-
...but noninteractive